

## Two-photon decay of the first excited $0^+$ state in $^{16}\text{O}$

A. C. Hayes\*

*Theoretical Physics Institute, School of Physics and Astronomy, University of Minnesota, Minneapolis, Minnesota 55455  
and Theoretical Division, Los Alamos National Laboratory, Los Alamos, New Mexico 87545*

J. L. Friar and D. Strottman

*Theoretical Division, Los Alamos National Laboratory, Los Alamos, New Mexico 87545*

(Received 20 November 1989)

Recent experiments observed unexpectedly strong interference between the  $E1$ - $E1$  and  $M1$ - $M1$   $2\gamma$  decay modes of the  $0^+$  (6.05 MeV) state in  $^{16}\text{O}$ . We present the results of a detailed calculation which evaluates the two-photon amplitude between realistic nonspurious many-body wave functions derived from a large basis  $\text{SU}(3)$  shell-model calculation, including up to  $5\hbar\omega$  of excitation. It is found that, as a result of strong cancellation between contributions to the transition polarizability from the giant dipole states built on the closed shell and the deformed (6.05 MeV)  $0^+$  state, the  $2E1$  matrix element is greatly suppressed. Since the standard one-body  $M1$  operator cannot excite the closed shell, strong cancellations are not seen in this case. The resulting  $2M1$  decay mode becomes competitive with the  $2E1$  decay, although it is still underestimated by the calculations.

### I. INTRODUCTION

A surprising result from the recent measurement<sup>1</sup> of the two-photon decay rate of the first excited  $0^+$  (6.05 MeV) state in  $^{16}\text{O}$  is the observed interference between  $E1$ - $E1$  and  $M1$ - $M1$  transitions, resulting from double  $E1$  and  $M1$  matrix elements of similar strength. Naively, one would expect the  $E1$ - $E1$  decay mode to dominate this process since the  $M1$ - $M1$  matrix element involves an operator of the order  $(1/Mc)^2$ . For example, the ground-state electric dipole polarizability and total magnetic susceptibility of  $^{16}\text{O}$  provide a direct measure of the diagonal matrix elements of the  $2E1$  and  $2M1$  operators involved in  $2\gamma$  decay, and there the  $2M1$  matrix element is observed<sup>2,3</sup> to be two orders of magnitude smaller than the  $2E1$  value. Indeed, ground-state magnetic susceptibilities are found<sup>3</sup> to be considerably smaller than electric polarizabilities throughout the nuclear mass table. Thus, there is much current interest in the question of how nuclear structure effects cause the  $M1$ - $M1$  transition to be competitive with the expected dominant  $E1$ - $E1$  mode of the  $2\gamma$  decay of the  $0^+$  (6.05 MeV) state in  $^{16}\text{O}$ .

The measured  $2E1$  matrix element, or equivalently, the transition electric dipole polarizability, is about a factor of 30 smaller than the ground-state polarizability. In contrast, the  $2\gamma$   $M1$ - $M1$  matrix element, i.e., the transition magnetic susceptibility, is observed to be similar in magnitude to the ground-state susceptibility. This suggests that the transition  $2E1$  matrix element involves strong cancellations, so that any calculation of the relative strengths of these electric and magnetic transitions must incorporate a detailed description of the structure of the initial and final  $0^+$  states.

In this work we present the results of a detailed calculation which evaluates the two-photon (nuclear Compton)

amplitude between realistic many-body wave functions. The nuclear wave functions used were derived from a large basis shell-model calculation. As is well known, the ground state of  $^{16}\text{O}$  is mainly described in terms of a closed  $p$  shell, whereas the  $0^+$  (6.05 MeV) state has a dominant  $4p$ - $4h$  structure. In addition,  $2p$ - $2h$  configurations play an important role in the structure of both these states. Thus, we have used a large  $(0+2+4)\hbar\omega$  basis to describe the initial and final states involved in this  $0^+ \rightarrow 0^+$  transition. The virtual  $1^+$  states appearing in the  $2M1$  matrix element were described using a  $(2+4)\hbar\omega$  model space. For the  $T=1; 1^-$  states involved in the  $2E1$  amplitude it was necessary to include up to  $5\hbar\omega$  of excitation. As discussed in detail below, this requirement results from the need to include the full dipole strength built on our model ground and deformed  $0^+$  wave functions. In addition, it is essential that any spurious center-of-mass states be eliminated from the basis, as these can give rise to large errors in the calculated polarizabilities.

Analysis of the two-photon matrix elements within our model shows a strong sensitivity of the calculated decay rate to the  $2p$ - $2h$  correlations in the ground-state wave function. The unexpectedly strong  $M1$ - $M1$  interference with the dominant  $E1$ - $E1$  decay mode can be understood as a consequence of both the properties of the operators involved and the structure of the initial and final wave functions. We find that, as a result of strong cancellation between contributions to the transition polarizability from the giant dipole states built on the deformed (6.05 MeV)  $0^+$  state and the ground state, the  $2E1$  matrix element is greatly suppressed. Since the closed  $p$  shell can make no contribution to the  $2\gamma$   $M1$ - $M1$  matrix element, strong cancellations are not seen in this case, and the resulting  $2M1$  decay mode becomes competitive with the  $2E1$  decay.

## II. CALCULATIONS

### A. Introduction

The gauge-invariant two-photon amplitude has been derived by Friar and Fallieros.<sup>4</sup> Only dipole gamma-gamma multiplicities are expected to be important, a result which is confirmed<sup>1</sup> by experiment, e.g.,  $\Gamma_{\gamma\gamma}(2E2)/\Gamma_{\gamma\gamma}(\text{total}) < 0.8\%$  for the  $^{16}\text{O}$  ( $0^+$ , 6.05 MeV) state. Limiting ourselves to dipole terms, the two-photon decay process is determined<sup>4</sup> by two observables; namely, the transition electric polarizability describing the  $2E1$  decay mode

$$\alpha_{E1}^f = 2 \sum_n \frac{\langle 0_f^+ | D_z | 1_n^- \rangle \langle 1_n^- | D_z | 0_i^+ \rangle}{\Delta E_n} \quad (1)$$

and the transition magnetic susceptibility  $\chi^f = \chi_D^f + \chi_P^f$  corresponding to the  $2M1$  matrix element. Here the diamagnetic susceptibility is

$$\chi_D^f = -\frac{Z}{6m} \langle 0_f^+ | r^2 | 0_i^+ \rangle \quad (2)$$

and the paramagnetic susceptibility is

$$\chi_P^f = 2 \sum_n \frac{\langle 0_f^+ | \mu_z | 1_n^+ \rangle \langle 1_n^+ | \mu_z | 0_i^+ \rangle}{\Delta E_n}. \quad (3)$$

The energy denominator is given by

$$-2\Delta E_n^{-1} = \frac{1}{(E_i - E_n + q_1)} + \frac{1}{(E_i - E_n + q_2)},$$

where  $q_1$  and  $q_2$  are the outgoing gamma-ray energies  $q_1 + q_2 = E_i - E_f$ . It is a good approximation to write  $q_1 \simeq q_2 \simeq \frac{1}{2}(E_i - E_f)$ , so that  $\Delta E_n \simeq [\frac{1}{2}(E_i + E_f) - E_n]$ , and we shall use this throughout these calculations.

The  $E1$  and  $M1$  operators appearing in (1) and (3) both transform simply under the SU(3) symmetries of the harmonic oscillator, i.e., the  $E1$  operator transforms as  $(\lambda, \mu) = (1, 0)$  for  $\Delta\hbar\omega = +1$ , while the one-body  $M1$  operator, which necessarily involves only  $\Delta\hbar\omega = 0$ , transforms as  $(\lambda, \mu) = (0, 0)$  for  $\Delta S = 1$ , and  $(\lambda, \mu) = (1, 1)$  for  $\Delta L = 1$ . Thus it is advantageous to perform our shell-model calculations in an SU(3) basis. The choice of basis for the intermediate (virtual)  $1^-$  and  $1^+$  states depends directly on the initial and final wave functions, and so we first discuss our model space for the  $0^+$  states.

### B. The positive-parity basis

There have been a number of studies<sup>5</sup> of the structure of the  $0^+$  states in  $^{16}\text{O}$ , and these indicate that the ground state is mainly a  $0\hbar\omega$  state, with 2p-2h  $2\hbar\omega$  configurations making up 10–20% of the wave function. In contrast, the  $0^+$  (6.05 MeV) state is described as primarily a 4p-4h

state having a large overlap with an  $\alpha + ^{12}\text{C}$  cluster configuration.

Our  $2\hbar\omega$  basis includes all possible SU(3) representations, i.e., the configurations with  $(\lambda, \mu) = (4, 2)$ ,  $(3, 1)$ ,  $(2, 0)$ ,  $(2, 3)$ ,  $(1, 2)$ ,  $(0, 1)$ ,  $(0, 4)$ , and  $(5, 0)$ , but has been restricted to include  $S = 0$  and  $S = 1$  states only. These  $2\hbar\omega$  configurations are all excitations of the type  $p^{10}(sd)^2$ , but to eliminate spurious center-of-mass (c.m.) states exactly we also included  $p^{11}(pf)$  and  $(0s)^{-1}p^{12}(sd)$  configurations.

The truncation of our  $4\hbar\omega$  basis was chosen so as to include the high  $(\lambda, \mu)$  representations which we expect to be dominant in a full  $4\hbar\omega$  calculation. For a harmonic oscillator  $\alpha + ^{12}\text{C}$  cluster state, with eight quanta of excitation associated with the relative motion wave function, the representations  $^{12}\text{C}((0, 4)) \times (8, 0) \rightarrow (\lambda, \mu) = (8, 4)$ ,  $(7, 3)$ ,  $(6, 2)$ ,  $(5, 1)$ , and  $(4, 0)$  are important. The two-body interaction favors the  $(8, 4)$  configuration, and diagonalization of the shell-model Hamiltonian shows that the (noncluster) representations with  $(\lambda, \mu) = (9, 2)$ ,  $(10, 0)$ , and  $(8, 1)$  are also important, but excitations with  $(\lambda, \mu) = (5, 1)$  and  $(4, 0)$  are found to make up only a very small fraction of the  $4\hbar\omega$  wave function. Thus, our  $4\hbar\omega$  basis includes all configurations with  $(\lambda, \mu) = (8, 4)$ ,  $(7, 3)$ ,  $(6, 2)$ ,  $(9, 2)$ ,  $(10, 0)$ , and  $(8, 1)$ . In addition to the dominant 4p-4h [ $p^8(sd)^4$ ] configurations we included excitations of the type  $p^9(sd)^2(pf)$ ,  $p^{10}(pf)^2$ ,  $p^{10}(sd)(sdg)$ , and  $(0s)^{-1}p^{10}(sd)^3$  [whenever they are allowed for one of the above  $(\lambda, \mu)$ ]. These additional basis states are essential for the elimination of spurious c.m. states.

Since the one-body  $M1$  operator is a  $\Delta\hbar\omega = 0$  operator we used the same truncation scheme for the virtual  $1^+$  states appearing in (3) as we did for the  $0^+$  wave functions. However, the  $(8, 4)$   $4\hbar\omega$  representation which dominates the  $0^+$  (6.05 MeV) wave function cannot contribute to the  $1^+$  wave functions, as in this case only  $L = \text{even}$ ,  $S = 0$ ,  $T = 0$  states are allowed. We note also that the number of ways of coupling to  $(\lambda, \mu) = (6, 2)$  is very large, and we thus chose to restrict our  $4\hbar\omega$  basis to include only those  $(6, 2)$  states with  $S = 0$ . This means that our  $1^+$  wave functions do not involve this representation.

### C. The $1^-$ ; $T = 1$ basis

The dominant contributions to  $\alpha_{E1}^f$  in the sum (1) come from the giant dipole  $1^-$  states built on the initial and final  $0^+$  states. If we write the  $0^+$  wave functions schematically as

$$0_{\text{g.s.}}^+ = \alpha |0\hbar\omega\rangle + \beta |2\hbar\omega\rangle + \gamma |4\hbar\omega\rangle \quad (4)$$

and

$$0_2^+ = \alpha' |0\hbar\omega\rangle + \beta' |2\hbar\omega\rangle + \gamma' |4\hbar\omega\rangle$$

we can express (1), using a closure approximation, as

$$\alpha_{E1}^f \simeq 2 \frac{4\pi}{9} \left[ \alpha\alpha' \frac{\langle 0\hbar\omega || E1 \cdot E1 || 0\hbar\omega \rangle}{\epsilon_1} + \beta\beta' \frac{\langle 2\hbar\omega || E1 \cdot E1 || 2\hbar\omega \rangle}{\epsilon_2} + \gamma\gamma' \frac{\langle 4\hbar\omega || E1 \cdot E1 || 4\hbar\omega \rangle}{\epsilon_3} + (\alpha\beta' + \beta\alpha') \frac{\langle 2\hbar\omega || E1 \cdot E1 || 0\hbar\omega \rangle}{\epsilon_4} + (\beta\gamma' + \gamma\beta') \frac{\langle 4\hbar\omega || E1 \cdot E1 || 2\hbar\omega \rangle}{\epsilon_5} \right]. \quad (5)$$

Here the  $\epsilon_i$ 's are the appropriate average energies whose values we will not consider as they do not affect our choice of  $1^-$  basis. The coefficients  $\alpha\alpha'$ ,  $\beta\beta'$ , and  $\gamma\gamma'$  are all comparable in magnitude, and, by orthogonality of the wave functions, introduce strong destructive interference between the  $\Delta\hbar\omega=0$  matrix elements. These cancellations are responsible for the large difference in magnitude between the ground-state (diagonal) polarizability and the transition polarizability, and are realized fully only if our  $1^-$  basis includes the complete dipole strength built on the  $0\hbar\omega$ ,  $2\hbar\omega$ , and  $4\hbar\omega$  states.

In determining the important contributions to the  $\Delta\hbar\omega=2$  matrix elements, we note that the  $\Delta L=0 E1 \cdot E1$  operator transforms as  $(\lambda, \mu)=(2, 0)$  in this case. Thus, the high  $(\lambda, \mu)$  representations in the  $2\hbar\omega$  and  $4\hbar\omega$  bases make no contribution to these. For example, the highest weight  $2\hbar\omega$  configuration,  $(\lambda, \mu)=(4, 2)$ , can connect via the double  $E1$  operator to

$$(4, 2) \times (2, 0) \rightarrow (6, 2), (5, 1), (4, 3), \dots$$

Hence, within our truncated  $4\hbar\omega$  basis, only the  $(6, 2)$  states contribute to the  $\Delta\hbar\omega=2$  matrix elements, and, since these representations are not favored by the interaction, the  $2\hbar\omega \rightarrow 4\hbar\omega$  matrix elements are small. In the case of the  $0\hbar\omega \rightarrow 2\hbar\omega$  matrix elements, only the  $(\lambda, \mu)=(2, 0)$   $2\hbar\omega$  states contribute. However, as we will discuss below, these  $(2, 0)$  components can make up a sizeable fraction of the  $0_{g.s.}^+$  wave function, and play a crucial role in determining the magnitude of  $\alpha_{E1}^i$ . For this reason we include the full dipole strength built on the  $(2, 0)$  representation, i.e., the full  $1\hbar\omega$  basis and the  $3\hbar\omega$  representations with  $(\lambda, \mu)=(3, 0)$  and  $(1, 1)$ .

Since the  $4\hbar\omega$  configurations with  $(\lambda, \mu)=(8, 4)$ ,  $(9, 2)$ , or  $(10, 0)$  cannot connect via the  $E1$  operator to any  $3\hbar\omega$  states, the dipole states built on these representations only involve  $5\hbar\omega$  configurations. Similarly, the dipole states built on the  $(\lambda, \mu)=(4, 2)$ ,  $(2, 3)$ ,  $(0, 1)$ ,  $(0, 4)$ , and  $(5, 0)$   $2\text{p-}2\text{h}$  configurations only involve  $3\hbar\omega$  excitations. Thus, in evaluating  $\alpha_{E1}^i$  it is imperative that our  $1^-$  basis contain large  $3\hbar\omega$  and  $5\hbar\omega$  bases, along with the usual  $1\text{p-}1\text{h}$  states. The truncation of these bases was chosen so as to include states which make a significant contribution to  $\alpha_{E1}^i$  and states which are favored by the two-body interaction. The  $3\hbar\omega$  representations included were those with  $(\lambda, \mu)=(6, 3)$ ,  $(5, 2)$ ,  $(7, 1)$ ,  $(2, 5)$ ,  $(4, 1)$ ,  $(3, 3)$ ,  $(3, 0)$ , and  $(1, 1)$ , and involved excitations of the type  $p^9(sd)^3$ ,  $p^{10}(sd)(pf)$ ,  $(0s)^{-1}p^{11}(sd)^2$ ,  $p^{11}(sdg)$ , and  $(0s)^{-1}(pf)$ . Our  $5\hbar\omega$  basis included the configurations  $p^7(sd)^5$ ,  $p^8(sd)^3(pf)$ ,  $(0s)^{-1}p^9(sd)^4$ ,  $p^9(sd)(pf)^2$ , and  $p^9(sd)^2(sdg)$  with  $SU(3)$  symmetry  $(\lambda, \mu)=(10, 2)$ ,  $(9, 4)$ ,  $(11, 0)$ ,  $(8, 3)$ , and  $(7, 5)$ .

#### D. The $0^+$ wave functions

Shell-model calculations which use empirically determined effective interactions produce quite reasonable descriptions of the structure of states of nuclei in the  $^{16}\text{O}$  mass region. This is especially true when multiparticle-multihole excitations are included, and the particle-hole ( $ph$ ) interaction often employed is that derived by Millener and Kurath<sup>6</sup> (MK). In conventional shell-model

calculations, such multi- $\hbar\omega$  excitations can introduce some inconsistencies, which are best illustrated with reference to our present calculations for  $^{16}\text{O}$ . These consistency problems are most apparent for the  $2\text{p-}2\text{h}$  and  $1\text{p-}1\text{h}$   $2\hbar\omega$  excitations,  $p^{-2}(sd)^2$ ,  $p^{-1}(pf)$ , and  $(0s)^{-1}(sd)$ , which couple to  $(\lambda, \mu)=(2, 0)$ . Standard effective interactions, including the MK  $ph$  interaction used here, contain no density dependence and no self-consistency for the single-particle wave functions. The lack of density dependence in the interaction causes the giant monopole resonance [ $ph$  pairs coupled to  $J=0$ ,  $S=0$ , and  $(\lambda, \mu)=(2, 0)$ ] to lie too low in energy. Mixing between the  $2\text{p-}2\text{h}$   $(2, 0)$  configurations and the closed shell is determined by the strongest part of the central interaction, i.e., by the  $\Delta\hbar\omega=2$  matrix elements which transform as  $(2, 0)$  under  $SU(3)$ . The large magnitude of these matrix elements leads to strong mixing between the  $2\text{p-}2\text{h}$  and the  $p^{12}$  configurations, and hence to a depression of the ground state by several MeV. The  $1\text{p-}1\text{h}$   $(2, 0)$  configurations couple to the closed shell through matrix elements of the kinetic energy operator ( $T$ ). The matrix elements of  $T$  are proportional to  $\hbar\omega$  and cancel with large contributions from the interaction. Hence the resultant off-diagonal matrix elements are poorly determined.

There is no clear prescription for handling the problems associated with the  $(2, 0)$  excitations, and so it is difficult to determine the amplitude of these configurations in the ground-state wave function. On the other hand, they play an important role in determining the total electric dipole strength built on the ground state. In light of this, we chose to calculate the  $2\gamma$  matrix elements as a function of the  $(2, 0)$  amplitude in the wave function, treating the strength of the  $(2, 0)$  interaction as a parameter. We note that these matrix elements also play a role in determining the mixing between the  $2\hbar\omega$   $(4, 2)$  and  $4\hbar\omega$   $(6, 2)$  configurations in our basis. We diagonalized our  $(0+2+4)\hbar\omega$  space using the Cohen-Kurath<sup>7</sup> (CK)  $p$  shell, Chung-Wildenthal<sup>8</sup>  $sd$  shell, and MK  $ph$  interactions, and varied the magnitude of the  $2\hbar\omega$   $(2, 0)$  matrix elements from zero to the full MK value, i.e.,  $V(2, 0)=\epsilon V_{\text{MK}}(2, 0)$ ,  $0 \leq \epsilon \leq 1$ . To correct for the large energy spacing obtained when  $\epsilon > 0$  between the ground state (mainly  $0\hbar\omega$ ) and the 2 and 4  $\hbar\omega$  states, we em-

TABLE I.  $0^+$  wave functions as a function of  $\epsilon$ .

$\epsilon$	$\Delta$ (MeV)	$J_n^\pi$	% $0\hbar\omega$	% $2\hbar\omega$	% $4\hbar\omega$
0.0	0.0	$0_1^+$	88.5	10.6	0.87
		$0_2^+$	2.5	3.8	93.7
0.25	0.6	$0_1^+$	84.85	14.0	1.15
		$0_2^+$	3.0	3.5	93.5
0.5	2.3	$0_1^+$	78.0	20.2	1.8
		$0_2^+$	3.8	3.4	92.8
0.75	5.0	$0_1^+$	69.0	28.3	2.7
		$0_2^+$	4.6	3.7	91.7
1.0	8.25	$0_1^+$	60.0	36.4	3.6
		$0_2^+$	5.1	4.7	90.2

ployed the prescription introduced by Ellis<sup>9</sup> for eliminating unlinked diagrams from shell-model calculations. In this method one adds a parameter  $\Delta$  to the unperturbed (diagonal)  $0\hbar\omega$  matrix element, where the value of  $\Delta$  is chosen so as to ensure that the ground-state energy is restored to its original ( $\epsilon=0$ ) position after diagonalization. For the  $p$ - and  $sd$ -shell single-particle energies we used the CK and MK values, respectively, and set  $\hbar\omega=13.0$  MeV.

Tables I and II list the  $0_{g.s.}^+$  and  $0^+$  (6.05 MeV) wave functions resulting from these calculations. The  $0\hbar\omega$  ( $2\hbar\omega$ ) amplitude in the ground state decreases (increases) as  $\epsilon$  varies from 0 to 1, and the strength of the closed-shell configuration ranges from 88.5% to 60% of the wave function. Equally notable is the change in SU(3) composition of the  $2\hbar\omega$  excitations as a function of  $\epsilon$ , where the total  $(\lambda,\mu)=(2,0)$  intensity in the ground state is 0.18% for  $\epsilon=0$  and 16.19% for  $\epsilon=1$ . The  $4\hbar\omega$  amplitude in the ground-state wave function varies from  $\gamma=0.093$  to 0.19, which compares well with the Brown and Green<sup>5</sup> value of 0.13. As expected, the  $(\lambda,\mu)=(8,4)$  4p-4h configuration is found to dominate the wave function of the  $0^+$  (6.05 MeV) state, reflecting the  $\alpha+^{12}\text{C}$  cluster structure of this state. The  $(2,0)$  2p-2h and the  $0p-0h$  amplitudes in the wave function increase with the strength of the  $\Delta\hbar\omega=2$  interaction, but the state is primarily ( $>90\%$ ) described in terms of  $4\hbar\omega$  excitations for all  $\epsilon$ .

The lowest-lying  $T=1$   $1^+$  state is predicted to be the  $(4,2)$  2p-2h state with  $L=2$ ,  $S=1$ , while the  $1_2^+$  state is the  $L=0$ ,  $S=1$   $(4,2)$  state. Analysis<sup>10</sup> of the two-particle transfer data to the analog states in  $^{16}\text{N}$  indicates that the  $L=2$  strength should be more equally shared between these two states. Fortunately, this shortcoming of the model wave functions does not greatly affect our predictions for the magnetic susceptibility as the energy denominator in Eq. (3) is similar for these two states. However, as will be discussed below, the  $M1$  strength to the  $1^+$  states in this excitation region is generally underestimated by the model. The first  $4\hbar\omega$   $T=1$   $1^+$  state is predicted to have a dominant  $(9,2)$   $L=1$ ,  $S=1$  structure and to lie at 4.5 MeV above the  $1^+$  (16.22 MeV) state.

#### E. The giant dipole resonances (GDR) built on the $0_{g.s.}^+$ and $0^+$ (6.05 MeV) state

To obtain some confidence in the  $T=1$   $1^-$  wave functions we first examined the lower-lying  $T=0$   $1^-$  states in  $^{16}\text{O}$ . The model predicts the  $T=0$   $1^-$  (7.11 MeV) level to be dominantly a  $(\lambda,\mu)=(2,1)$   $p^{-1}(sd)$  state. The electron scattering form factor<sup>11</sup> for excitation of this state is characteristic of a  $(2,1)$   $p \rightarrow (sd)$  transition; however, to reproduce the observed  $|F_L(q)|^2$  within a pure  $1\hbar\omega$  model requires the use of large effective charges and oscillator parameter. The second  $T=0$   $1^-$  level at 9.63 MeV is known<sup>5</sup> to be the lowest member of the  $Q=9$   $\alpha+^{12}\text{C}$   $K=0^-$  band (where  $Q$  is the number of oscillator quanta associated with the relative motion wave function of the cluster system). In shell-model terms this corresponds to a  $5\hbar\omega(\lambda,\mu)=(9,4)$  [ $p^7(sd)^5+p^8(sd)^3(pf)$ ] band. Because our  $5\hbar\omega$  space is strongly truncated we do not obtain

TABLE II. Intensities of SU(3)  $(\lambda,\mu)$  components in the  $0^+$  wave functions.

$\epsilon$	(0,0)	(4,2)	(3,1)	(2,0)	(2,3)	(1,2)	(0,1)	(0,4)	(5,0)	(8,4)	(7,3)	(9,2)	(8,1)	(10,0)	(6,2)
0.0	88.5	9.8	0.4	0.2	0.03	0.01	0.0	0.01	0.24	0.75	0.04	0.05	0.01	0.0	0.01
	2.5	3.0	0.3	0.13	0.02	0.0	0.0	0.0	0.42	76.6	4.8	9.1	0.6	1.4	1.2
0.25	84.9	11.2	0.5	2.0	0.04	0.0	0.01	0.04	0.29	0.94	0.05	0.06	0.01	0.0	0.10
	3.03	2.75	0.23	0.06	0.02	0.0	0.0	0.02	0.4	76.33	4.74	9.1	0.63	1.39	1.3
0.5	78.05	13.15	0.61	5.83	0.05	0.02	0.04	0.15	0.36	1.24	0.07	0.08	0.01	0.0	0.35
	3.76	2.55	0.18	0.16	0.01	0.01	0.01	0.05	0.38	75.74	4.72	9.03	0.63	1.38	1.37
0.75	68.98	15.6	0.8	10.94	0.06	0.06	0.09	0.32	0.46	1.63	0.1	0.11	0.01	0.01	0.83
	4.56	2.42	0.15	0.55	0.01	0.03	0.02	0.12	0.36	74.77	4.66	8.92	0.62	1.37	1.44
1.0	60.0	17.83	1.0	16.19	0.07	0.1	0.14	0.49	0.53	1.86	0.12	0.12	0.01	0.10	1.52
	5.08	2.65	0.12	1.22	0.01	0.06	0.04	0.21	0.38	73.41	4.57	8.73	0.61	1.34	1.56

enough binding for these states. To correct for this we added a (negative) constant to all the diagonal  $5\hbar\omega$  matrix elements in order that after diagonalization of the Hamiltonian the  $(9,4)$   $1^-$  state lay at 9.6 MeV of excitation. The  $1^-$  at 12.43 MeV is then predicted to be the first  $3\hbar\omega$  state and has a dominant  $(6,3)$  structure.

For the  $T=1$   $1^-$  states we added the same constant to the diagonal  $5\hbar\omega$  matrix elements as used in the  $T=0$  case. The model predicts the 13.1 MeV  $1^-$   $T=1$  state to be almost a pure ( $>99\%$ )  $1\hbar\omega$  state, with a dominant  $(\lambda,\mu)=(2,1)$  structure. The  $1\hbar\omega$  giant dipole  $1p-1h$   $(1,0)$  state is concentrated around 25-MeV excitation, and the lowest-lying  $3\hbar\omega$   $T=1$  state is predicted at 19.5 MeV. Figures 1 and 2 show the distribution of dipole strength predicted in the present model for the ground state and  $0^+$  (6.05) state, respectively. [Our  $1^-$  basis involves 272 nonspurious states; however, in these figures we show the dipole strength to a given  $1^-$  state only if the calculated  $B(E1:0^+ \rightarrow 1^-)$  value is greater than  $10^{-4} e^2 \text{fm}^2$ .] As  $\epsilon$  ranges from 0 to 1 the change in 2p-2h structure of the ground-state wave function (Tables I and II) results in a significant change in predicted distribution of dipole strength. For example, the average energy

$$\left[ \bar{E}_{E1} \equiv \frac{\sum_n B(E1:0^+ \rightarrow 1^-) \cdot E_x}{\sum_n B(E1:0^+ \rightarrow 1^-)} \right]$$

of the giant resonance built on the ground state is  $\bar{E}_{E1} = 25.1$  MeV for  $\epsilon=0$  and  $\bar{E}_{E1} = 30.0$  MeV for  $\epsilon=1$ .

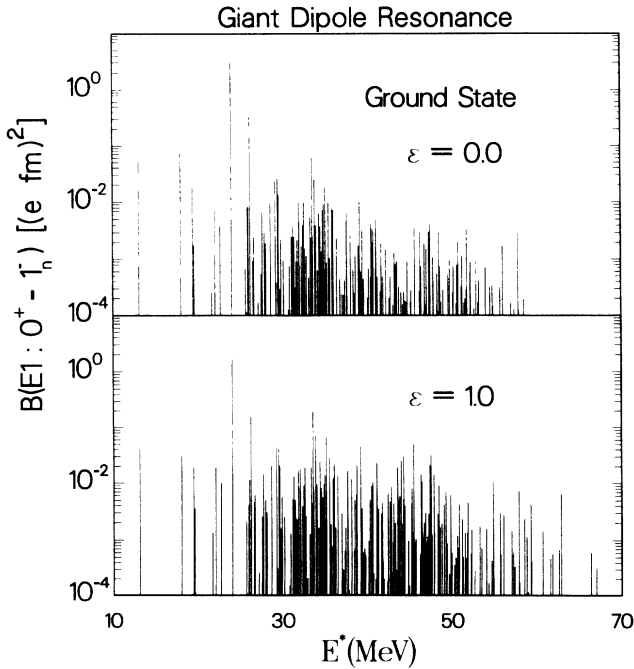


FIG. 1. The  $B(E1:0^+_{g.s.} \rightarrow 1^-)$  strength as a function of the excitation energy of the intermediate  $1^-$  states. Results are shown for two values of the  $(\lambda,\mu)=(2,0)$   $\Delta\hbar\omega=2$  two-body interaction;  $\epsilon=0$  and  $\epsilon=1$ . The transition strengths are given in units of  $e^2 \text{fm}^2$ .

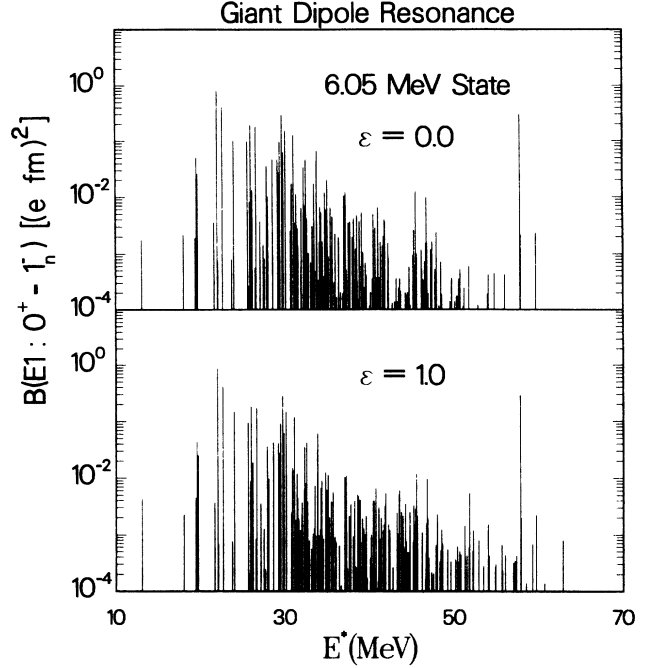


FIG. 2. As for Fig. 1, but for the  $0^+$  (6.05 MeV) state.

We find the giant resonance built on the  $4p-4h$   $0^+$  (6.05 MeV) to be more fragmented in energy than that built on the ground state. For a pure  $(8,4)$   $0^+$  state the  $E1$  operator can excite  $5\hbar\omega$   $1^-$  states with  $SU(3)$  symmetry  $(\lambda,\mu)=(9,4)$ ,  $(7,5)$ , and  $(8,3)$ . Our shell-model calculations predict the  $(9,4)$   $1^-$  state to be concentrated at 22 MeV of excitation, but a sizeable (9%) contribution to the total dipole strength, from an  $(8,3)$  state, is predicted at 57.0 MeV. Since the  $(9,4)$  state lies so low in energy it mixes strongly with the  $1p-1h$  states (via  $3p-3h$  states), even though these two configuration differ by  $4\hbar\omega$  of excitation. A large fraction of the strength built on the deformed state lies close in energy to that built on the ground state, and 63% of the energy-weighted sum rule is predicted below 30 MeV. The  $E1$  transition strength to the  $0^+$  (6.05 MeV) state has been studied<sup>12</sup> via the  $^{15}\text{N}(p,\gamma_1)^{16}\text{O}$  reaction, and the cross section is found to peak at 24.0 MeV of excitation; however, the cross section for this reaction is also determined by the single-particle ( $\Gamma_p$ ) and total ( $\Gamma$ ) widths of the  $1^-$  states involved, so that a direct comparison of Figs. 1 and 2 with the observed cross section could be misleading.

### III. The $2\gamma$ MATRIX ELEMENTS

#### A. The transition polarizability

In Table III we list our results for the transition and ground-state dipole polarizabilities as a function of  $\epsilon$ , where, as described in Sec. IID,  $\epsilon$  determines the strength of the  $\Delta\hbar\omega=2$   $(2,0)$  interaction. As the  $2\hbar\omega$   $(2,0)$  amplitude in the ground-state wave function increases, the magnitudes of both  $\alpha_{E1}^p$  and  $\alpha_{E1}^g$  decrease considerably, and we find the inclusion of these ground-state correlations necessary in order to reproduce the observed

TABLE III. Two-photon matrix elements<sup>a,b</sup> (in units of  $10^{-3}$  fm<sup>3</sup>).

$\epsilon$	$\alpha_{E1}^f$	$\alpha_{E1}^{g,s}$	$\chi_P^f$	$\chi_P^{g,s}$
0.0	-43.2	700	0.86	0.48
0.25	-37.4	652	0.92	0.6
0.5	-29.0	600	0.97	0.86
0.75	-18.9	550	1.1	1.27
1.0	-8.9	508	1.3	1.53
Expt.	$-17 \pm 4$	585	$\chi_P + \chi_D = 2.7 \pm .7$ $ \chi_D _{\text{expt}} = 0.91$ $\chi_{D,\text{theory}} < 0$	1.78

<sup>a</sup>No effective charges were used in calculating the dipole polarizabilities, and the oscillator parameter  $b = 1.7$  fm was used.

<sup>b</sup>Bare  $g$  factors were used to calculate the magnetic susceptibilities.

polarizabilities. Incorporating these (2,0) excitations into the ground state leads to destructive interference between the  $0\hbar\omega \rightarrow 1\hbar\omega$  (GDR) and  $2\hbar\omega \rightarrow 1\hbar\omega$  (GDR) amplitudes. This is not unexpected, and can be understood in terms of the extended schematic model of Brown.<sup>13</sup> There it is shown that, for repulsive interactions, the inclusion of ground state correlations results in a decrease in the total transition probability and an increase in the excitation energy of the resonant state.

To understand the large difference in magnitude between  $\alpha_{E1}^f$  and  $\alpha_{E1}^{g,s}$  seen both experimentally<sup>1</sup> and theoretically, we call on the schematic Eqs. (4) and (5). As a result of orthogonality of the initial and final  $0^+$  wave functions, the first three terms in (5) add destructively in the case of the transition polarizability, giving us a small  $\Delta\hbar\omega=0$  contribution to  $\alpha_{E1}$ . In contrast, these three terms add constructively for the ground-state polarizability, yielding the total  $\Delta\hbar\omega=0$   $E1$  strength for the ground state. The fifth term in (5) is small for both  $\alpha_{E1}^{g,s}$  and  $\alpha_{E1}^f$  because, as discussed in Sec. II C, the dominant  $4\hbar\omega$  configurations cannot connect to the  $2\hbar\omega$  states via the  $E1 \cdot E1$  operator. However, the  $0\hbar\omega \rightarrow 2\hbar\omega$  matrix element plays an important role in determining the magnitude of  $\alpha_{E1}^f$ , and from Table III we see that varying the  $2\hbar\omega$  components of the ground-state wave function leads to large changes in the predicted magnitude of the transition polarizability. To display this more clearly we list in Table IV the individual diagonal and  $\Delta\hbar\omega=2$  contributions to  $\alpha_{E1}^f$ . As the ground-state correlations are increased these two contributions become comparable in magnitude and strongly cancel one another. Thus, we find that the small magnitude of the observed transition polarizability can be explained by two separate cancella-

TABLE IV. Contribution to  $\alpha_{E1}$  (in units of  $10^{-3}$  fm<sup>3</sup>).

$\epsilon$	$\Delta\hbar\omega=0$	$\alpha_{E1}^f$	$\Delta\hbar\omega=2$	$\Delta\hbar\omega=0$	$\alpha_{E1}^{g,s}$	$\Delta\hbar\omega=2$
0.0	-37.3		-5.9	707.0		-7.0
0.5	-43.7		14.7	682.2		-30.2
1.0	-42.8		33.9	634.5		-126.5

tions; namely (i) destructive interference between the three  $\Delta\hbar\omega=0$  matrix elements appearing in (5), and (ii) strong cancellation between the resultant  $\Delta\hbar\omega=0$  and the off-diagonal  $\Delta\hbar\omega=2$  matrix elements. In the case of the ground-state polarizability only this second cancellation occurs, and the calculated value is quite sensitive to the (2,0) amplitudes in the ground-state wave function, but  $\alpha_{E1}^{g,s}$  remains about a factor of 20–50 larger than  $\alpha_{E1}^f$ , depending on the value of  $\epsilon$ .

Earlier estimates<sup>1,14</sup> of the  $2\gamma$  matrix elements involved two-state mixing models and assumed the  $\Delta\hbar\omega=2$  contributions in (5) to be negligible. However, the present work indicates that these ground-state correlations play an important role in determining the magnitude of both the transition and ground state dipole polarizabilities, and that models which do not include  $2\hbar\omega$  excitations will tend to overestimate the  $2E1$  transition probability.

### B. The transition magnetic susceptibility $\chi_{M1}$

The seagull contribution to the  $2M1$  decay mode  $\chi_D$  [Eq. (2)] is difficult to calculate reliably because of the strong cancellations which occur when evaluating monopole matrix elements with harmonic oscillator wave functions. We thus chose to use the observed<sup>11</sup> value of  $\langle r^2 \rangle$  (obtained from inelastic electron scattering), and to take its relative sign from our shell-model estimate. This gives  $\chi_D = -0.91 \times 10^{-3}$  fm<sup>3</sup>.

Our results for the transition paramagnetic susceptibility [Eq. (3)] are summarized in Table III. Here we see that, as the ground-state correlations are increased, both  $\chi_P^f$  and  $\chi_P^{g,s}$  increase. In the case of the double  $M1$  matrix element the schematic closure approximation of Eqs. (4) and (5) reduces to

$$\chi_{M1}^f \approx 2 \frac{4\pi}{9} \left[ \beta\beta' \frac{\langle 2\hbar\omega || M1 \cdot M1 || 2\hbar\omega \rangle}{\epsilon} + \gamma\gamma' \frac{\langle 4\hbar\omega || M1 \cdot M1 || 4\hbar\omega \rangle}{\epsilon'} \right]. \quad (6)$$

The term involving  $\alpha\alpha'$  in (5) is zero because the  $M1$  operator cannot excite the closed shell, and, if we restrict ourselves to the standard one-body operator, the  $\Delta\hbar\omega=2$  matrix elements are also zero. The  $2\hbar\omega \rightarrow 2\hbar\omega$  and  $4\hbar\omega \rightarrow 4\hbar\omega$  contributions to  $\chi_P$  add constructively and increasing  $\beta$  increases the total  $M1$  strength built on the ground state.

We find  $\chi_P$  and  $\chi_D$  to be of opposite sign, so that the calculations underestimate the  $2M1$  matrix elements. To understand this result we must examine the model predictions for the single-photon  $M1$  strength to the low-lying  $1^+ T=1$  states. In Table V we list these transition strengths for  $\epsilon=0$  and  $\epsilon=1$ , and it is clear that the model underestimates them considerably. In addition, the predicted  $B(M1)$  value is quite sensitive to the structure of the ground-state wave function (Figs. 3 and 4), and we see an order of magnitude difference in the  $B(M1:1^+ \rightarrow 0^+)$  value for these two values of  $\epsilon$ , whereas the  $2\hbar\omega$  intensity in the ground-state wave function changes by a factor of 3. This sensitivity of the  $M1$  strength to the structure of

TABLE V.  $M1$  transition strengths from the  $1^+$   $T=1$  states to the ground state of  $^{16}\text{O}$ .

$J_n^\pi(E_x)$	$B(M1:1^+ \rightarrow 0^+)$ in units of $\mu_N^2$				PSD <sup>a</sup>	ZBM <sup>a</sup>
	Experiment <sup>a</sup>	$\epsilon=1$	$\epsilon=0$			
$1_1^+(16.22 \text{ MeV})$	$0.075 \pm 0.01$	0.01	0.001	0.002	0.218	
$1_2^+(17.14 \text{ MeV})$	$0.116 \pm 0.017$	0.028	0.006	0.004	0.095	
$1_3^+(18.8 \text{ MeV})$	$0.043 \pm 0.01$	0.008	0.0004	0.016	0.01	
% $2\hbar\omega$ in ground state		36.4	10.6	21	25	

<sup>a</sup>K. A. Snover *et al.*, Phys. Rev. C **27**, 1837 (1983). PSD and ZBM are the interactions derived in Refs. 6 and 19, respectively.

the ground state has been studied by Arima and Strottman<sup>15</sup> and is most easily understood in terms of the spatial symmetry of the wave function. The dominant symmetry in the ground-state wave function is  $[f]=[4^4]$   $T=0$ ,  $S=0$ , and the total  $M1$  strength to this configuration is identically zero (assuming the standard one-body operator). The  $[f]=[4^322]$  configuration is the next most favored symmetry, but it also cannot connect to the  $1^+$   $T=1$ ,  $S=1$  states whose wave functions are dominated by  $[4^331]$  symmetry. The MK  $ph$  interaction strongly favors high spatial symmetries, and thus  $M1$  strength from the ground state to the low-lying  $1^+$   $T=1$  states in  $^{16}\text{O}$  arises from small admixtures in the wave functions. It has been shown by Arima and Strottman<sup>15</sup> and by Snover *et al.*<sup>16</sup> that use of an interaction which largely breaks the particle symmetry, such as the ZBM<sup>19</sup> interaction, leads to strong  $M1$  transition strengths to the low-lying  $1^+$  states.

An alternate solution to the problem of underpredicted isovector magnetic dipole strength in  $^{16}\text{O}$  may lie in the need for an effective  $M1$  operator. Corrections to the

single-particle  $M1$  operator arising from meson-exchange currents, core polarization, and isobar currents have been calculated by Towner and Khanna.<sup>17</sup> These corrections have also been studied by Brown and Wildenthal<sup>18</sup> (BW) from detailed comparisons of  $0\hbar\omega$  shell-model predictions with measured transition strengths, and an empirically optimum  $M1$  operator was deduced for the  $sd$  shell. If we write the one-body  $M1$  operator as

$$M1 = \sqrt{3/4\pi}(g_L L + g_S S + g_P \sqrt{8\pi}[Y_2 \times S]^{(1)}), \quad (7)$$

the free-nucleon values for an isovector transition correspond to  $g_L=0.5$ ,  $g_S=4.706$ ,  $g_P=0.0$ , while the BW values for  $A=17$  are  $g_L^{\text{eff}}=0.591$ ,  $g_S^{\text{eff}}=4.12$ , and  $g_P^{\text{eff}}=0.32$ . Towner and Khanna deduced  $g$  factors for an effective one-body  $M1$  operator, which reproduce their two-body corrections to the Schmidt magnetic moments, and for  $A=15$  and  $A=17$  they are close to the BW values.

The  $[Y_2 \times S]^{(1)}$  term appearing in (7) does not conserve the particle symmetry and can connect large components in the wave functions directly. We calculated the  $M1$  transition strengths to the  $1^+$  ( $T=1$ ) states in  $^{16}\text{O}$  using the effective  $M1$  operator of Brown and Wildenthal.<sup>18</sup>

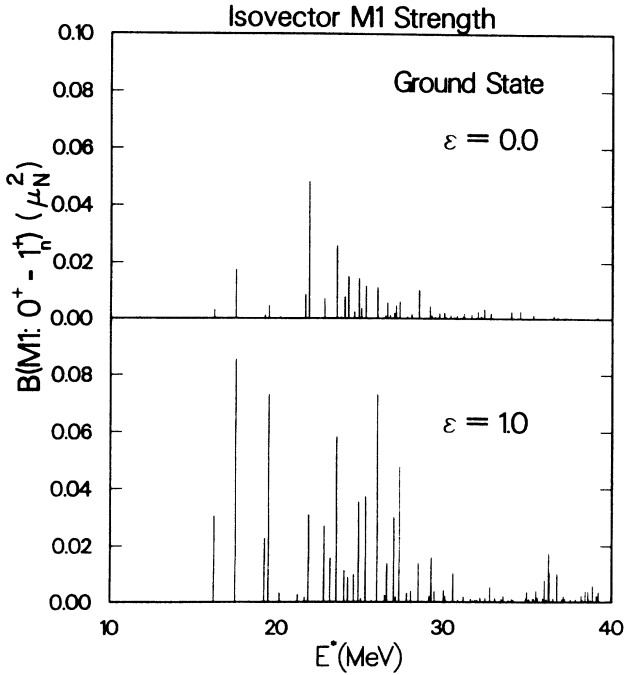


FIG. 3. The ground-state  $M1$  strength for two values of (2,0) interaction strength;  $\epsilon=0$  and  $\epsilon=1$ .  $E_x$  corresponds to the excitation energy of the intermediate  $1_n^+$  states, and the  $B(M1)$  values are given in units of  $\mu_N^2$ .

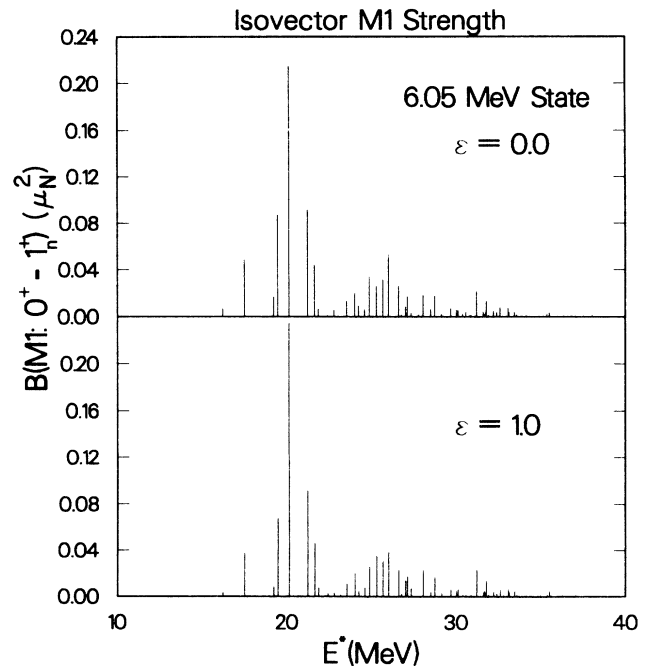


FIG. 4. As for Fig. 3, but for the  $0^+$  (6.05 MeV) state.

We obtained as much as a factor of two in the  $B(M1)$  value for some weak transitions, but the total isovector  $M1$  strength built on the ground state only increased by 4.5% to 17%, depending on the value of  $\epsilon$ . For some individual transitions the effective operator leads to quenching of the  $M1$  matrix element, but the summed strength to all  $1^+$  ( $T=1$ ) states was enhanced. We note that the effective operator we used was not derived for states which differ from the ground state by  $2\hbar\omega$  of excitation, and that there remains uncertainty regarding the structure of the ground-state wave function. In light of this, it is difficult to draw conclusions on the poor comparison between the predicted and observed  $B(M1)$  values to the  $1^+$  ( $T=1$ ) states between 16–18 MeV of excitation in  $^{16}\text{O}$ . However, it does seem clear that our underestimation of the  $2\gamma$   $M1$ - $M1$  matrix element is directly related to the lack of the single-photon isovector  $M1$  strength predicted by the model.

#### IV. SUMMARY

Two-photon decay of excited states is one of the basic second-order electromagnetic processes seen in nuclei. The results of the recent measurements<sup>1</sup> of  $2\gamma$  decay of  $0^+ \rightarrow 0^+$  transitions in  $^{16}\text{O}$ ,  $^{40}\text{Ca}$ , and  $^{90}\text{Zr}$ , where the  $2M1$  matrix elements were observed to be of the same order of magnitude as the  $2E1$ , were quite unexpected. Indeed, from  $\sum_{-2}$  cross-section measurements it is known<sup>3</sup> that  $(\chi_{M1}/\alpha_{E1})^{e.s.} < 10^{-2}$ , throughout the mass table. To understand the large difference between these diagonal matrix elements and the transition matrix elements measured in the  $0^+ \rightarrow 0^+$  decays we have examined in detail the  $2\gamma$  decay of the  $0^+$  (6.05 MeV) state in  $^{16}\text{O}$ .

$^{16}\text{O}$  has the advantage of being well suited to an  $SU(3)$  shell-model description. Using the  $SU(3)$  scheme we could describe the wave functions,  $2\gamma$  operators and the two-body effective interaction within a consistent framework, taking advantage of their symmetry properties to simplify our results. The  $2E1$  operator involves both a  $\Delta\hbar\omega=0$  and  $\Delta\hbar\omega=2$  term, which transform under  $SU(3)$  as  $(\lambda, \mu)=(0,0)$  and  $(\lambda, \mu)=(2,0)$ , respectively. In calculating the  $2M1$  matrix element we restricted ourselves to a one-body  $M1$  operator (i.e., to a  $\Delta\hbar\omega=0$  operator).

In evaluating the transition polarizability it was necessary to include the full electric dipole strength built on both the ground state and the deformed state, in order to reproduce the strong cancellation seen in the  $2E1$  matrix element. This meant using a large  $(1+3+5)\hbar\omega$   $1^-$  basis to describe the intermediate  $T=1$   $1^-$  states. Truncation of the basis and the elimination of spurious center of mass states was achieved by exploiting the  $SU(3)$  symmetry properties of the wave functions.

The suppression of the transition polarizability was found to arise from strong cancellation between the different  $\Delta\hbar\omega=0$  matrix elements, i.e., contributions to  $\alpha_{E1}^{e.s.}$  from the giant dipole resonance built on the closed shell added destructively with those from the resonance built on the 2p-2h and 4p-4h states. There was then a further cancellation between this total  $\Delta\hbar\omega=0$  and the  $\Delta\hbar\omega=2$  contributions to the  $2E1$  matrix element. In the case of the ground-state polarizability the  $\Delta\hbar\omega=0$  contri-

butions add constructively, and although there was cancellation between the  $\Delta\hbar\omega=0$  and  $\Delta\hbar\omega=2$  matrix elements, the resultant value of  $\alpha_{E1}^{e.s.}$  remained about a factor of 30 larger than  $\alpha_{E1}^{f.}$

The  $\Delta\hbar\omega=2$   $(\lambda, \mu)=(2,0)$  part of the effective two-body interaction is not well determined, and so we calculated the  $2\gamma$  matrix elements as a function of the strength of this interaction. We found the magnitude of both  $\alpha_{E1}^{e.s.}$  and  $\alpha_{E1}^{f.}$  to have a strong dependence on the ground-state correlations, i.e., on the  $2\hbar\omega$  (2,0) amplitude in the ground-state wave function. In particular, the calculations show that, as the (2,0) amplitude increases, there is a large decrease in predicted dipole polarizabilities, which results from the destructive interference between the  $\Delta\hbar\omega=0$  and  $\Delta\hbar\omega=2$  matrix elements. This is not surprising, and reflects the need to include 2p-2h configurations in any realistic description of the ground state and the deformed 6.05 MeV  $0^+$  state in  $^{16}\text{O}$ . Indeed, our calculations suggest that two state mixing models which omit these 2p-2h excitations should have difficulty reproducing the unexpectedly small  $2E1$  matrix element.

There are two contributions to the  $2M1$  decay, namely the paramagnetic and the diamagnetic susceptibility. The magnitude of the diamagnetic term is given in terms of the monopole matrix element  $\langle 0_f^+ | r^2 | 0_i^+ \rangle$ , which is known<sup>11</sup> from electron scattering, and the sign of which was determined from our shell-model estimates. The paramagnetic susceptibility was calculated using a large  $(2+4)\hbar\omega$  shell-model basis for the intermediate  $T=0$  and  $T=1$   $1^+$  states. Our calculations showed that only the  $T=1$  states make a significant contribution to the  $2M1$  matrix element. We found  $\chi_P$  and  $\chi_D$  to be of opposite sign for both the ground state and the transition susceptibilities, and that the model predictions for  $\chi_P$  were too small by about a factor of 3. This underprediction of the  $2M1$  matrix element appears to be directly related to the well known problem of underpredicted (single-photon) isovector  $M1$  strength in  $^{16}\text{O}$ . To estimate meson exchange current, isobaric current, and core polarization effects on these  $M1$  transitions, we calculated the  $2M1$  matrix elements using an effective  $M1$  operator, which was deduced<sup>17,18</sup> in order to reproduce these two-body effects in this mass region. Use of an effective operator did increase the predicted  $2M1$  matrix elements; however, the total isovector strength built on the ground state was not enhanced enough to explain the experimental  $M1$  nor  $M1$ - $M1$  strengths. The lack of predicted  $M1$  strength is probably due largely to the fact that the two-body interaction used strongly favors the particle symmetry of the wave functions.

Although the calculations underestimate the  $2M1$  strength, they do indicate that this decay mode should be competitive with the  $2E1$  decay. Indeed, we found that the  $2M1$  matrix element did not involve strong cancellations, such as those seen in the  $2E1$  case. This is mainly because the one-body (effective or standard)  $M1$  operator cannot excite the closed shell, so that the  $\Delta\hbar\omega=0$  contributions to  $\chi_P$  add constructively. Thus, the ground state and the transition magnetic susceptibilities are predicted to be similar in strength, in agreement with experiment.



Furthermore, if we restrict ourselves to a one-body  $M1$  operator, the  $2M1$  matrix element does not involve a  $\Delta\hbar\omega=2$  component, which in the  $2E1$  case lead to further destructive interference. Use of an effective  $M1$  operator suggests that  $\Delta\hbar\omega=2$  contributions to the  $2M1$  decay would not be large and would enhance the transition probability, but without carrying out full calculations of these effects it is difficult to draw strong conclusions on this point.

Processes which involve excitation via two or more electromagnetic interactions are now becoming more viable probes of the nucleus. The present work suggests that microscopic evaluation of the gauge-invariant nuclear Compton amplitude between many-body wave functions can lead to a satisfactory understanding of the experiments. The interesting and unexpected results from

the recent measurement of  $0^+ \rightarrow 0^+$  two-photon decays suggest exciting prospects for two-photon (and multiphoton) interactions in nuclear physics.

#### ACKNOWLEDGMENTS

One of us (A.C.H.) wishes to thank D. J. Millener for his help on many aspects of this problem, and is grateful to P. J. Ellis and H. T. Fortune for valuable discussions. A.C.H. was supported in part by fellowships from the University of Minnesota Theoretical Physics Institute and SuperComputer Institute, and by Department of Energy (DOE) Contract No. DE-FG02-87ER40328. The work of J.L.F and D.S. was performed under the auspices of the U.S. Department of Energy.

\*Present address: Theoretical Division, Los Alamos National Laboratory, Los Alamos, NM 87545.

<sup>1</sup>J. Kramp, D. Habs, R. Kroth, M. Music, J. Schirmer, D. Schwalm, and C. Broude, Nucl. Phys. **A474**, 412 (1987).

<sup>2</sup>W. Knupfer and A. Richter, Z. Phys. **A 320**, 473 (1985).

<sup>3</sup>J. Ahrens, H. Gimm, A. Zieger, and B. Ziegler, Nuovo Cimento **32A**, 364 (1976); W. Knupfer and A. Richter, Phys. Lett. **101B**, 375 (1981).

<sup>4</sup>J. L. Friar, Ann. Phys. (NY) **95**, 170 (1975); J. L. Friar and S. Fallieros, Phys. Rev. C **34**, 2029 (1986).

<sup>5</sup>G. E. Brown and A. M. Green, Nucl. Phys. **75**, 401 (1966); Y. Suzuki, Prog. Theor. Phys. **55**, 1751 (1976); **56**, 111 (1976); Y. Suzuki and B. Imanishi, Phys. Rev. C **23**, 2414 (1981).

<sup>6</sup>D. J. Millener and D. Kurath, Nucl. Phys. **A255**, 315 (1975).

<sup>7</sup>S. Cohen and D. Kurath, Nucl. Phys. **73**, 1 (1965).

<sup>8</sup>W. Chung, Ph.D. thesis, Michigan State University, 1976 (unpublished).

<sup>9</sup>P. J. Ellis, in *Windsurfing the Fermi Sea*, edited by T. T. S. Kuo and J. Speth (Elsevier, Amsterdam, 1987), Vol. II.

<sup>10</sup>H. T. Fortune (private communication).

<sup>11</sup>T. N. Buti, J. Kelly, W. Bertozzi, J. M. Finn, F. W. Hersman, C. Hyde-Wright, M. V. Hynes, M. A. Kovash, S. Kowalski, R. W. Lourie, B. Murdock, B. E. Norum, B. Pugh, C. P. Sargent, W. Turchinets, and B. L. Berman, Phys. Rev. C **33**, 755 (1986).

<sup>12</sup>D. P. Balamuth, K. D. Brown, T. Chapuran, and C. M. Laymon, Phys. Rev. C **36**, 2235 (1987).

<sup>13</sup>G. E. Brown, *Unified Theory of Nuclear Models and Forces*, 2nd ed. (North-Holland, Amsterdam, 1971).

<sup>14</sup>G. F. Bertsch, Part. Nucl. **4**, 237 (1972).

<sup>15</sup>A. Arima and D. Strottman, Phys. Lett. **96B**, 23 (1980).

<sup>16</sup>K. A. Snover, G. E. Adelberger, P. G. Ikossi, and B. A. Brown, Phys. Rev. C **27**, 1837 (1983).

<sup>17</sup>I. S. Towner and F. C. Khanna, Nucl. Phys. **A339**, 334 (1983).

<sup>18</sup>B. A. Brown and B. H. Wildenthal, Nucl. Phys. **A474**, 290 (1987); Phys. Rev. C **28**, 2397 (1983).

<sup>19</sup>A. P. Zucker, B. Buck, and J. B. McGrory, Phys. Rev. Lett. **21**, 39 (1968).